



King's Research Portal

DOI:

[10.3390/app12020874](https://doi.org/10.3390/app12020874)

[Link to publication record in King's Research Portal](#)

Citation for published version (APA):

Weber, C., Bonini, N., Wei, Y., Plekhanov, E., Zhao, Z., MacHeda, F., & Tse, T. (2022). High-Temperature Superconductivity in the Lanthanide Hydrides at Extreme Pressures. *Applied Sciences (Switzerland)*, 12(2), 12. Article 874. <https://doi.org/10.3390/app12020874>

Citing this paper

Please note that where the full-text provided on King's Research Portal is the Author Accepted Manuscript or Post-Print version this may differ from the final Published version. If citing, it is advised that you check and use the publisher's definitive version for pagination, volume/issue, and date of publication details. And where the final published version is provided on the Research Portal, if citing you are again advised to check the publisher's website for any subsequent corrections.

General rights





Copyright and moral rights for the publications made accessible in the Research Portal are retained by the authors and/or other copyright owners and it is a condition of accessing publications that users recognize and abide by the legal requirements associated with these rights.

- Users may download and print one copy of any publication from the Research Portal for the purpose of private study or research.
- You may not further distribute the material or use it for any profit-making activity or commercial gain
- You may freely distribute the URL identifying the publication in the Research Portal

Take down policy

If you believe that this document breaches copyright please contact librarypure@kcl.ac.uk providing details, and we will remove access to the work immediately and investigate your claim.

High temperature superconductivity in the lanthanide hydrides at extreme pressures

Yao Wei ¹ , Francesco Macheda ¹ , Zelong Zhao ¹, Terence Tse ¹, Evgeny Plekhanov ^{1,*} , Nicola Bonini ^{1,*}  and Cedric Weber ^{1,*}

¹ King's College London, Theory and Simulation of Condensed Matter (TSCM), The Strand, London WC2R 2LS, UK; yao.wei@kcl.ac.uk

* Correspondence: evgeny.plekhanov@kcl.ac.uk; nicola.bonini@kcl.ac.uk; cedric.weber@kcl.ac.uk

Abstract: Hydrogen-rich superhydrides are promising high- T_c superconductors, with superconductivity experimentally observed near room temperature, as shown in recently discovered lanthanide superhydrides at very high pressures, e.g. LaH₁₀ at 170 GPa and CeH₉ at 150 GPa. Superconductivity is believed to be closely related with the high vibrational modes of the bound hydrogen ions. Here we study the limit of extreme pressures (above 200 GPa) where lanthanide hydrides with large hydrogen content have been reported. We focus on LaH₁₆ and CeH₁₆, two prototype candidates for achieving a large electronic contribution from hydrogen in the electron-phonon coupling. In this work, we propose a first-principles calculation platform with the inclusion of many-body corrections to evaluate the detailed physical properties of the Ce-H and La-H systems and to understand the structure, stability and superconductivity of these systems at ultra-high pressure. We provide a practical approach to further investigate conventional superconductivity in hydrogen rich superhydrides. We report that density functional theory provides accurate structure and phonon frequencies, but many-body corrections lead to an increase of the critical temperature, that is associated with spectral weight transfer of the f-states.

Keywords: superconductivity; electronic interactions; high pressure

1. Introduction

In the research of condensed matter [1], pressure is a fundamental thermodynamic variable that determines the state of matter, and plays an important role in the field. The discovery of new materials and thence application to industrial use makes up an important part of modern innovation. As a basic thermodynamic parameter, pressure demonstrates the ability to activate semi-core electrons, empty orbitals, and non-atom-centered quantum orbitals on interstitial sites, changing a given element's chemistry, and thus resulting in a plethora of novel and previously unexpected occurrences, for example the generation of new types of functional materials that deviate from those under atmospheric pressure (101.325 kPa) [2].

Currently, hydrogen-rich materials have garnered much attention in regards to obtaining superconductivity at high temperatures, and has led to much theoretical and experimental work on the search for high-temperature superconductivity of hydrides under high pressure [3]. The chemical pre-compression method, proposed by Neil Ashcroft in 2004, has led to the key realization that hydrogen-rich compounds are a new potential class of high-temperature superconductors [4]. As investigating the high-temperature superconductivity of metallic hydrogen is highly challenging [5], most scholars have instead redirected focus to the synthesis and properties of hydride-rich compounds instead. Recently, the realization of very high temperature superconductivity, at near room temperature, was discovered in hydrogen disulfide [6,7] and lanthanum hydrogen [8–10] an important set of milestones.

Citation: Lastname, F.; Lastname, F.; Lastname, F. Title. *Journal Not Specified* **2021**, *1*, 0. <https://doi.org/>

Received:

Accepted:

Published:

Publisher's Note: MDPI stays neutral with regard to jurisdictional claims in published maps and institutional affiliations.

Copyright: © 2022 by the authors. Submitted to *Journal Not Specified* for possible open access publication under the terms and conditions of the Creative Commons Attribution (CC BY) license (<https://creativecommons.org/licenses/by/4.0/>).

37 Hydrogen disulfide was previously believed to undergo dissociation under high
38 pressures, and was not heavily considered as a potential superconductor. However,
39 recent theoretical work has suggested that the dissociation would not occur, but that
40 on the contrary the material becomes superconducting [11]. Inspired by this discovery,
41 Drozdov et al. compressed sulfur hydride in a diamond anvil cell, and has shown that
42 hydrogen sulphide would indeed form a superconductor when compressed with a T_c of
43 up to 200 K [12].

44 Armed with this new knowledge, researchers have expanded their search to include
45 lanthanide hydrides under pressure, with notable examples such as La-H[13] and Y-
46 H[14]. The Fermi density and thus superconductivity in La-H systems are determined
47 not only by the d orbital La electrons and the s orbital H electrons, but also by the f
48 orbital electrons of lanthanum [15].

49 Using DFT, studies have found that the face-centered cubic (FCC) form of LaH₁₀ is
50 a good metal, with various bands crossing the Fermi level that forms a high electronic
51 density at the Fermi level [16]. In contrast, for the YH₁₀ system, only the d orbital Y
52 electrons and the s orbital H electrons become major contributors to the Fermi density
53 at high pressures [17]. As external pressure destabilizes the localised La- $4f$ more than
54 the other orbitals (La- $6s$, La- $5d$), the latter populates when pressure is applied, leading to
55 possible novel emergent quantum states associated with the strong electronic correlations.
56 In particular, it was purported that the La-H system has a unique high- T_c with f electrons
57 at the Fermi level. [18].

58 The effects of electronic localization and hybridization apply for all high-density
59 compounds, and is a hallmark for a wide family of similar materials signified by transi-
60 tion metals, lanthanides, and rare earth elements. Many-body effects give rise to a num-
61 ber of unique and interesting phenomena in similar systems, such as high-temperature
62 superconductivity in cuprates and the metal-insulator transition in vanadates at ambient
63 temperature [19]. The Zaanen-Sawatsky-Allen theory offers a categorization of transition
64 metal periodic solids in terms of their correlation' strengths, and has provided a good
65 knowledge base, though deep understanding of the hydride's characteristics distant
66 from ambient conditions remains hitherto difficult and incomplete [20].

67 Therefore, in order to identify new hydrogen-rich high- T_c superconductors at the
68 lowest possible pressure, the use of quantitative theoretical computations are required.
69 Superconductivity in these potential compounds are mediated by the interaction between
70 highly intense lattice vibrations of hydrogen atoms and the localised electrons. An
71 accurate description of this interaction necessitates fine descriptions of the electronic
72 characteristics, which are infamous for being difficult for such correlated f systems,
73 treating both itinerant and localised electrons on the same footing.

74 Several theoretical aspects, including the electron-phonon coupling strength λ ,
75 phonon dispersion relations, electron spectral weight, and cross terms between electron-
76 electron, and electron-phonon interactions are corrected with electronic correlations.

77 Here, we propose a pragmatic first-principles calculation consistent platform that
78 uses many-body corrections for the electronic spectral weight, which then feeds into
79 adjusted estimates of T_c . The many-body corrections to phonon dispersion are typically
80 less drastic than the corrections to the electronic spectra, as correlations effects can shift
81 the f -spectral weight over several eV. Furthermore, since their full treatment is beyond
82 reach, the scope of this work is restricted to only correcting the electronic spectra.

83 In this manuscript, we show that the many-body corrections in f orbital systems
84 could cause significant changes, with spectral weight shifts in the order of one electron
85 volt. We evaluate the precise physical properties of La-H and Ce-H systems, giving
86 special care to the effect of correlations on spectral properties. We find that LaH₁₆ and
87 CeH₁₆ have stable P6/mmm space group crystal structures at pressures up to 250 GPa.
88 Additionally, for the recently discovered Cerium hydride, we predict a comparatively
89 high T_c , evaluated using our pre-established hierarchical approach [21].

90 2. Discussion

91 The idea that hydrogen-rich compounds could be potential high T_c superconductors
92 dates back to the turn of the millennium, when chemical pre-compression was proposed
93 as a viable way to reduce the metallization pressure of hydrogen in the presence of other
94 elements, leading to observed T_c exceeding 150 K in the LaH₁₆ system. This indicates
95 compressed hydrogen-rich compounds as potential room-temperature superconductors.

96 The genesis of superconductivity in these hydrides is known to originate from
97 electron-phonon interactions. The characteristic phonon frequency, the electron-phonon
98 coupling strength, the density of states at Fermi level, and the Coulomb pseudopotential
99 μ^* are the four factors that define T_c according to BCS theory. Density functional
100 theory, using conventional pseudo-potentials, such as PBE, is widely acknowledged
101 to provide an accurate explanation of lattice dynamics. However, for compounds
102 with weakly hybridized and localized f electrons, such as La and Ce, where many-
103 body corrections are required, DFT is known to have difficulties in dealing with strong
104 electronic correlations.

105 We apply a density functional theory technique combined with dynamical mean-
106 field theory (DMFT) in this study. The charge and spin local fluctuations, which are
107 important for the local paramagnetic moment of lanthanide elements, are readily cor-
108 rected by DMFT. DMFT is used to account for changes in orbital character at the Fermi
109 surface caused by spectral weight transfer related with Hubbard f band splitting. This
110 influences low energy electron-electron scattering processes via phonon momentum
111 transfer, as stated in the Methods section, according to the Allen-Dynes formalism.

112 P6/mmm-LaH₁₆ and P6/mmm-CeH₁₆ shows very little dependence on pressure at
113 a hundred GPa. The phonon DOS of P6/mmm-LaH₁₆ and P6/mmm-CeH₁₆ computed at
114 250 GPa is shown in Fig. 1, panels (a) and (b). Then, we investigate the impact of various
115 DMFT electronic charge self-consistency schemes (see Fig. 1(c) and Fig. 1(d)). We find
116 that correlation effects have a significant impact on $\alpha^2F(\omega)$. In particular, we compare:
117 i) PBE density functional theory, ii) DFT+DMFT with the full charge self-consistent
118 formalism (DFT+DMFT+CSC). We used the Koster-Slater interaction vertex for the La
119 and Ce correlated manyfold, with typical values for $U = 6$ eV, $J = 0.6$ eV. Interestingly,
120 the full charge self-consistent DMFT provides a large increase of the superconducting
121 temperature (see panels (e) and (f) in Fig. 1). This confirms that many-body effects
122 have a sizeable contribution to the prediction of the superconducting temperatures in
123 lanthanide hydrides. Note that we use $U = 6$ eV, $J = 0.6$ eV throughout the rest of the
124 paper.

125 We focus on the LaH₁₆ and CeH₁₆ P6/mmm systems at 250 GPa. Although DMFT
126 readily provides important corrections to the electronic structure, it is worth investi-
127 gating how DMFT affects structural qualities. Calculating forces with limited atomic
128 displacement is not tractable due to the high computing overhead of doing many-body
129 adjustments. Recently, we have developed a method for calculation of forces within
130 DMFT, allowing for ultra-soft and norm-conserving pseudopotentials in the underlying
131 DFT [22]. This opens up new possibilities for systems with heavy components that are
132 not well-suited to all-electron computations. The structure relaxation at 250 GPa is seen
133 in Fig. 2. Typically, we obtain corrections for the bond lengths of the order of 5%.

134 The many-body effects tend to slightly shorten the La-H and Ce-H bonds, somehow
135 increasing the La-H and Ce-H covalency. At the same time, this La-H and Ce-H bond
136 length reduction is accompanied by a moderate increase in the H-H distance. This
137 behaviour is opposite to what we have previously found in CeH₉, where both Ce-H and
138 H-H bonds were longer within DMFT treatment [21].

139 The changes highlighted above stem directly from a spectral weight transfer in-
140 duced by many-body corrections (see Fig. 3(a) and 3(b)). In DFT, the La system is
141 described by a two band system in absence of long-range magnetic order. We note
142 that DFT is a single Slater determinant approach, and hence cannot capture the role of
143 paramagnetism, with an associated magnetic multiplet (fluctuating magnetic moment).

144 Such effects typically induce a splitting of spectral features into satellites, as observed
 145 in Figs. 3(c) and 3(d), with a resulting large increase of f character at the Fermi level.
 146 As sharp La features occur near the Fermi level, we emphasize that a higher level of
 147 theory is required to capture correctly the superconducting properties. For instance,
 148 in our calculations the one-shot (DFT+DMFT) and full charge self-consistent approach
 149 (DFT+DMFT+CSC) induces a small shift of the sharp La feature at the Fermi level, which
 150 in turns mitigates the f character increase at the Fermi level.

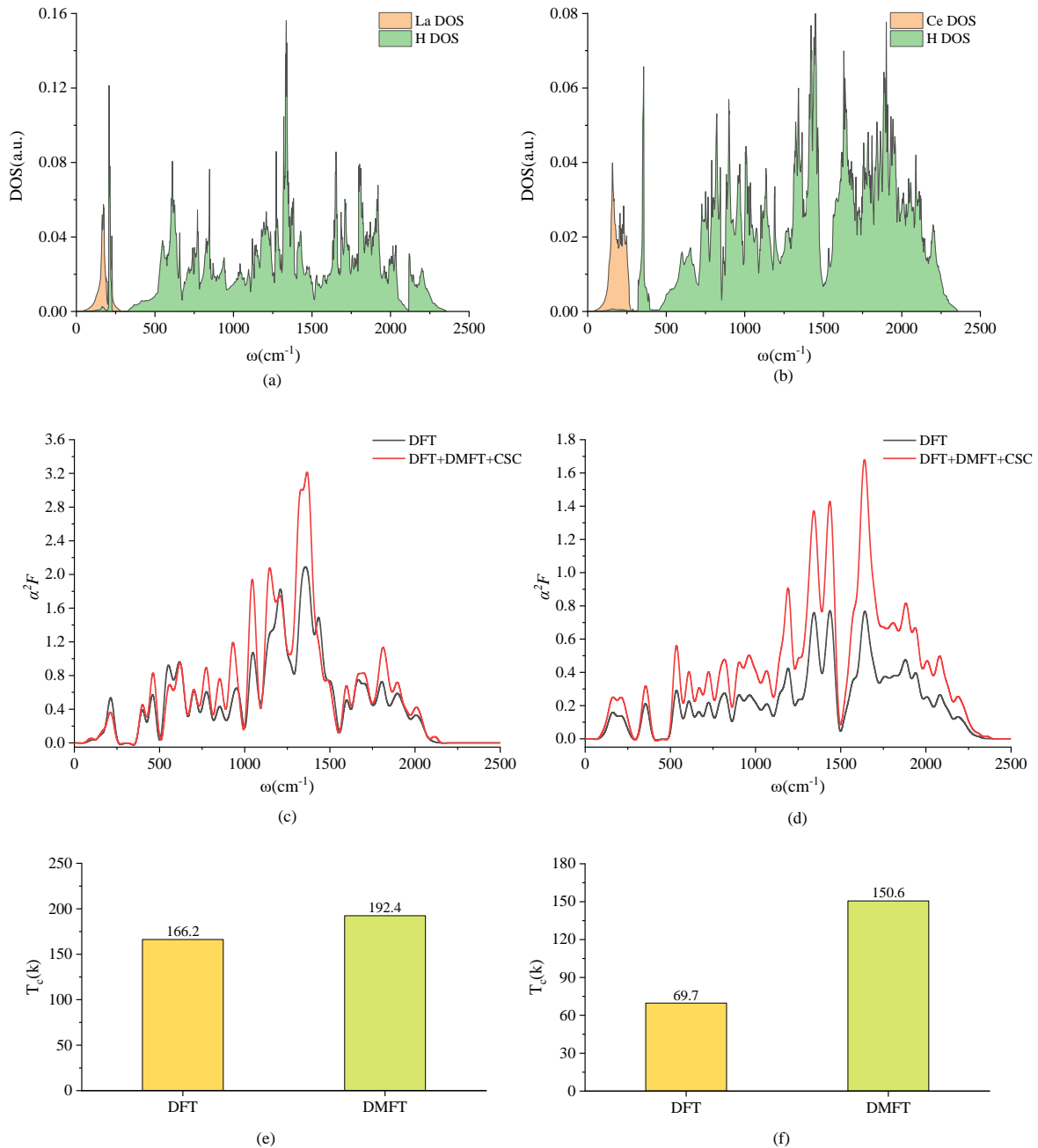


Figure 1. Many-body corrections to the superconducting temperature. We report (a) phonon density of states for LaH₁₆, (b) phonon density of states for CeH₁₆, (c) and (d) Eliashberg function $\alpha^2F(\omega)$ for LaH₁₆ and CeH₁₆, the spectral weight at the Fermi level is obtained at different levels of approximation: i) DFT PBE (black line), and ii) with the full charge self-consistent formalism (DFT+DMFT+CSC, red line). (e) and (f) the superconducting temperature T_c obtained by the Allen and Dynes formalism for LaH₁₆ and CeH₁₆ at 250 GPa. We obtain a theoretical estimate for LaH₁₆ is $T_c = 166.2$ K by DFT and $T_c = 192.4$ K by DMFT, also a theoretical estimate for CeH₁₆ is $T_c = 69.7$ K by DFT and $T_c = 150.6$ K by DMFT. The full charge self-consistent DMFT provides a large increase of the superconducting temperature, and the physical value of the Hund's coupling for La and Ce is $U = 6$ eV, $J = 0.6$ eV. All calculations were performed in the P6/mmm phase of LaH₁₆ and CeH₁₆ at 250 GPa.

151 The role of f orbitals appears to be very important for the superconducting proper-
 152 ties in rare-earth hydrates [21]. That is why in the present paper, in addition to LaH_{16}
 153 with formally empty La f shell, we study also Cerium hydrate (CeH_{16}) with one f
 154 electron in the atomic Ce configuration. We have checked that both systems remain
 155 stable at pressure up to at least 250 GPa.

156 We report in Fig. 4 the DFT+DMFT+CSC framework applied to CeH_{16} in the
 157 $P6/mmm$ phase at 250 GPa. We attribute the decrease in T_c to a higher f occupation,
 158 which shifts the chemical potential away from the f spectral features present near the
 159 Fermi level (see Fig. 4(c) and Fig. 4(d)). Furthermore, figure 4(b) shows that there is no
 160 obvious sudden change at Fermi level, but there is an obvious mutation at Fermi level in
 161 figure 4(d), which is around $7(1/\text{eV})$, the correction of DMFT greatly affected the T_c of
 162 Ce.

163 Our findings point to a possible path for increasing T_c in lanthanide hydrides: an
 164 increase in f character at the Fermi level in DFT+DMFT, which is associated with a lower
 165 degree of La-H and Ce-H covalency and a lower degree of hybridization, which, in turns,
 166 is a marker for a higher superconducting temperature in these systems.

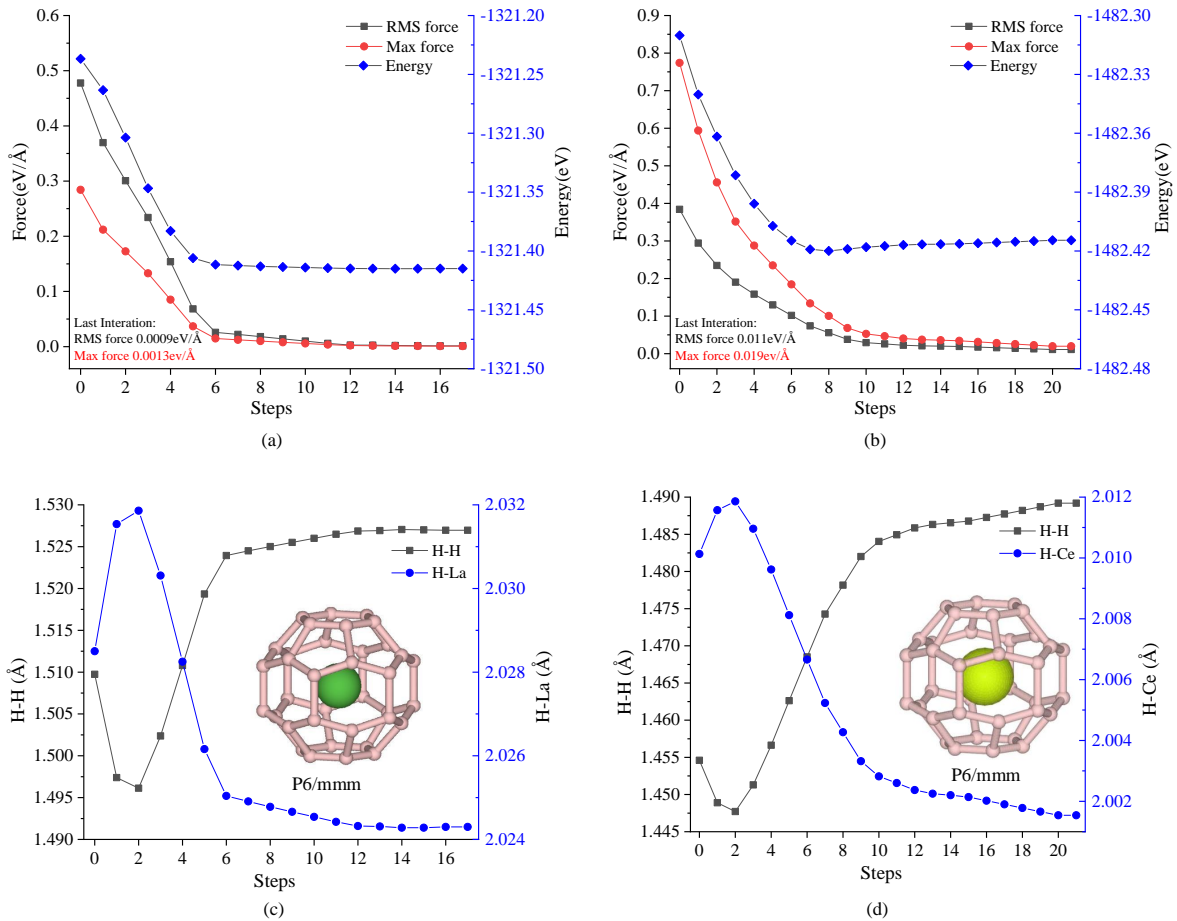


Figure 2. Structural relaxation of clathrate lanthanides with many-body corrections. We report the structural relaxation of the LaH_{16} (panel a and c) and prototype CeH_{16} (panel b and d) compounds. All calculations are performed at 250 GPa. The volume density is obtained by the equation of state in DFT+DMFT+CSC that provides very similar results to PBE (not shown). Internal coordinates are relaxed with DFT+DMFT+CSC, building upon the recent implementation of DFT forces for ultra-soft pseudo-potentials. We report the forces and total energies obtained during the structural optimization, respectively, in panel (a) (b) for LaH_{16} (CeH_{16}). Convergence is obtained within 25 iterations. The shortest H-H and Ce-H bond lengths increase throughout the structural optimization (see panel c and d for La and Ce hydrides, respectively).

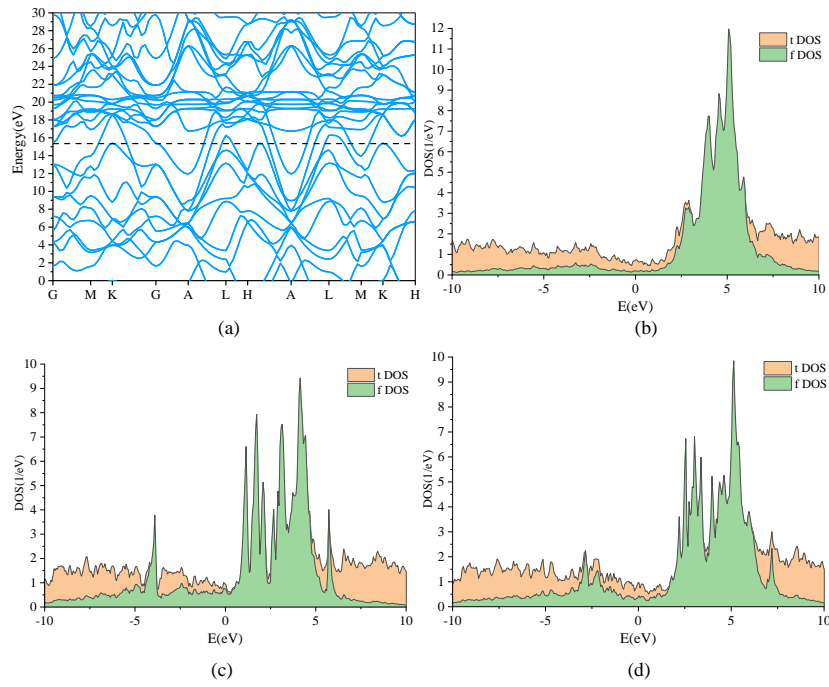


Figure 3. Spectral weight transfer induced by many-body corrections.(a) Electronic band structure and (b) density of states obtained by DFT calculations. *tDOS* and *fDOS* denote the spectral weight obtained by the imaginary part of respectively the lattice and *f* impurity Green function, corresponding to the spectral weight traced over all orbitals and traced over the *f* orbitals, respectively. In (c) and (d) we show the energy-resolved spectral weight, obtained respectively by the one-shot DFT+DMFT and the full charge self-consistent DFT+DMFT+CSC. All calculations were performed in the P6/mmm phase of LaH₁₆ at 250 GPa.

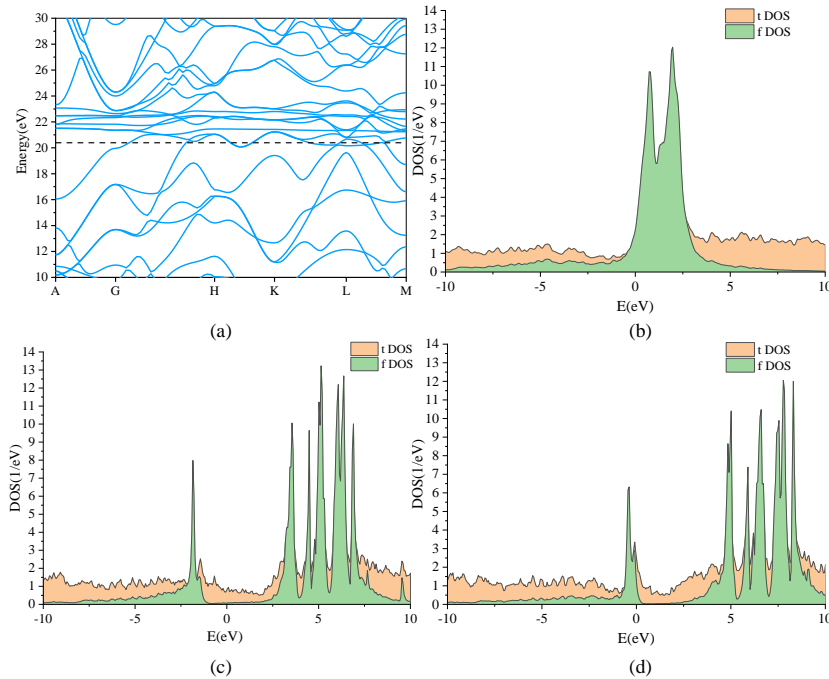


Figure 4. Spectral weight transfer induced by many-body corrections.(a) Electronic band structure and (b) density of states obtained by DFT calculations. *tDOS* and *fDOS* denote the spectral weight obtained by the imaginary part of respectively the lattice and *f* impurity Green function, corresponding to the spectral weight traced over all orbitals and traced over the *f* orbitals, respectively. In (c) and (d) we show the energy-resolved spectral weight, obtained respectively by the one-shot DFT+DMFT and the full charge self-consistent DFT+DMFT+CSC. All calculations were performed in the P6/mmm phase of CeH₁₆ at 250 GPa.

167 3. Methods

168 Figure 5 depicts our theoretical approach. We present a schematic overview of the
 169 theoretical platform's principal elements and their interrelationships. Our method
 170 establishes a modular framework for high-pressure material screening. Firstly, Crystal
 171 structure AnaLYsis by Particle Swarm Optimization (CALYPSO) provides stoichiometric
 172 compositions via Gibbs enthalpies for the equation of state and convex hull [23]. Inter-
 173 operability between Quantum Espresso(QE) [24,25] is accomplished through input file
 174 format conversion, pseudopotentials, and k-point grids. The many-body corrections are
 175 provided by core libraries via the DMFT quantum embedding, which results in corrected
 176 forces[22] and total free energies[26,27].

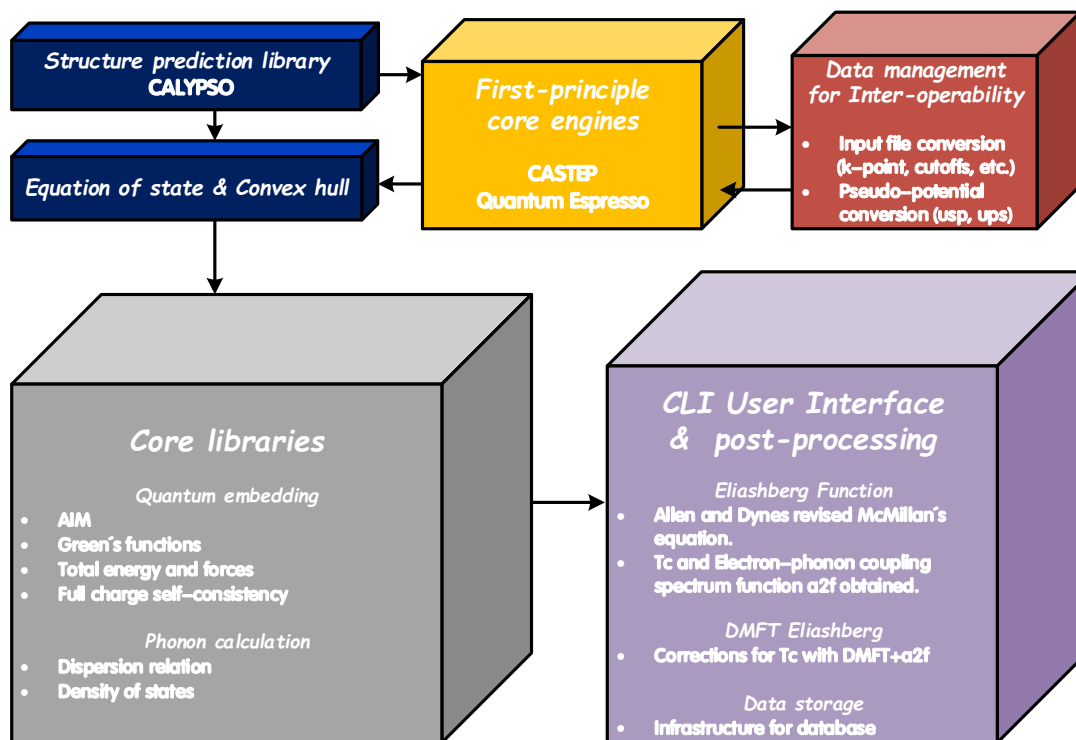


Figure 5. DFT inter-operability for a consistent many-body platform. Schematic overview of the main modules of the theoretical platform and its interrelations. Firstly, structures are predicted by Crystal structure AnaLYsis by Particle Swarm Optimization (CALYPSO)), via Gibbs enthalpies for the equation of state and convex hull. The underlying core engines are the CASTEP and Quantum Espresso DFT software. Inter-operability between QE and CASTEP is achieved via format conversion of input files, pseudo-potentials and k-point grids. Core libraries are used to provide the many-body corrections, via quantum embedding, which in turns provides corrected forces and energies. In post-processing, the Eliashberg function and superconducting T_c are obtained with the DMFT+a_{2F} approach. Finally, data are archived for future usage in hdf5.

177 The underlying structure relaxations were carried out using the QE and CASTEP
 178 packages in the framework of DFT and using PBE-GGA (Perdew-Burke-Ernzerhof
 179 generalized gradient approximation) [28,29]. Norm conserving pseudopotential were
 180 used to describe the core electrons and their effects on valence orbitals[30]. Valence
 181 electron configuration of $5s^25p^65d^16s^2$, $5s^25p^64f^15d^16s^2$ (i.e., with explicitly included
 182 f electrons) and $1s^1$ was used for the La, Ce and H atoms, respectively. A plane-
 183 wave kinetic-energy cut-off of 1000 eV and dense Monkhorst-Pack k-points grids with
 184 reciprocal space resolution of $12 \times 12 \times 12$ were employed in the calculation.

185 Phonon frequencies and superconducting critical temperature were calculated us-
 186 ing density-functional perturbation theory as implemented in QE [31]. The k-space
 187 integration (electrons) was approximated by a summation over a $20 \times 20 \times 12$ uni-
 188 form grid in reciprocal space, with the Methfessel-Paxton smearing scheme, using a

189 temperature of $k_B T = 0.05$ eV for self-consistent cycles and relaxations; the same grid
 190 ($20 \times 20 \times 12$) was used for evaluating DOS and coupling strength. Dynamical matrices
 191 and λ were calculated on a uniform $5 \times 5 \times 3$ grid in \mathbf{q} -space for P6/mmm-LaH₁₆ and
 192 P6/mmm-CeH₁₆.

193 In post-processing, the superconducting transition temperature T_c was estimated
 194 using the Allen-Dynes modified McMillan equation [32]:

$$T_c = \frac{\omega_{\log}}{1.2} \exp \left[\frac{-1.04(1 + \lambda)}{\lambda - \mu^*(1 + 0.62\lambda)} \right] \quad (1)$$

where μ^* is the Coulomb pseudopotential. The electron-phonon coupling strength λ
 and ω_{\log} were calculated as:

$$\omega_{\log} = \exp \left[\frac{2}{\lambda} \int \frac{d\omega}{\omega} \alpha^2 F(\omega) \log(\omega) \right], \quad (2)$$

$$\lambda = \sum_{\mathbf{q}\nu} \lambda_{\mathbf{q}\nu} = 2 \int \frac{\alpha^2 F(\omega)}{\omega} d\omega. \quad (3)$$

195 In the Allen-Dynes formalism, the Eliashberg function $\alpha^2 F(\omega)$ is obtained by sum-
 196 ming over all scattering processes at the Fermi level mediated by phonon momentum
 197 transfer and reads [33]:

$$\alpha^2 F(\omega) = N(\epsilon_F) \frac{\sum_{\mathbf{k}_1, \mathbf{k}_2} |M_{\mathbf{k}_1, \mathbf{k}_2}|^2 \delta(\omega - \omega_{\mathbf{q}\nu}) \delta(\epsilon_{\mathbf{k}_1}) \delta(\epsilon_{\mathbf{k}_2})}{\sum_{\mathbf{k}_1, \mathbf{k}_2} \delta(\epsilon_{\mathbf{k}_1}) \delta(\epsilon_{\mathbf{k}_2})}. \quad (4)$$

Here, $N(\epsilon_F)$ is the DOS at Fermi level, $\omega_{\mathbf{q}\nu}$ is the phonon spectrum of a branch ν at
 momentum $\mathbf{q} = \mathbf{k}_2 - \mathbf{k}_1$, $\epsilon_{\mathbf{k}_1}$ and $\epsilon_{\mathbf{k}_2}$ are electronic band energies referred to the Fermi
 level, while $M_{\mathbf{k}_1, \mathbf{k}_2}$ are the electron-phonon coupling matrix elements. Many-body effects
 introduce a change of spectral character at the Fermi level, where electronic correlations
 induce a mass enhancement and introduce a finite lifetime, due to incoherence. In this
 spirit of the DMFT scissors, we correct the DFT bands with the renormalised DMFT
 band picture:

$$\alpha^2 F(\omega) = \mathcal{A}_{tot} \frac{\sum_{\mathbf{k}_1, \mathbf{k}_2} |M_{\mathbf{k}_1, \mathbf{k}_2}|^2 \delta(\omega - \omega_{\mathbf{q}\nu}) \mathcal{A}(\mathbf{k}_1) \mathcal{A}(\mathbf{k}_2)}{\sum_{\mathbf{k}_1, \mathbf{k}_2} \mathcal{A}(\mathbf{k}_1) \mathcal{A}(\mathbf{k}_2)}, \quad (5)$$

198 where \mathcal{A}_{tot} and $\mathcal{A}(\mathbf{k})$ are respectively the total and \mathbf{k} -momentum resolved spectral
 199 weights at Fermi level. This approach is denoted as *DMFT+a2F* in the workflow.

200 Within the DFT+DMFT quantum embedding approach, the DFT Kohn-Sham eigen-
 201 states are used in the calculation of the DMFT Green function [21,34]. We use atomic
 202 projectors to define the Anderson Impurity Model (AIM), which is successively solved
 203 within the Hubbard-I approximation. A breadth of quantum solvers is readily available
 204 in the TRIQS open-source platform [35,36]. In the full charge self-consistent approach
 205 (DFT+DMFT+CSC), the Kohn-Sham potentials are calculated from the DMFT electronic
 206 density, obtained using the DMFT occupancies. Upon DMFT convergence, total energies
 207 and forces are calculated using the Green function and self-energy. All DFT calculations
 208 in this work are carried out using the pseudopotential formalism.

209 4. Conclusions

210 We created a methodology for estimating the superconducting temperature in
 211 lanthanide hydrides with many-body corrections, and investigated a novel type of stable
 212 high-temperature superconducting material, CeH₁₆. The DMFT charge self-consistency,
 213 which involves many-body adjustments to the local charge density in first-principles
 214 calculations, is used to restore a consistent theoretical framework. A change in the
 215 spectral weight of the f states causes a rise in predicted superconducting temperature,

216 which influences the spectral character at the Fermi level. In this research, we obtain a
217 theoretical estimate for LaH16 is $T_c = 166.2\text{K}$ by DFT and $T_c = 192.4\text{K}$ by DMFT, also
218 a theoretical estimate for CeH16 is $T_c = 69.7\text{K}$ by DFT and $T_c = 150.6\text{K}$ by DMFT, also
219 discussed the capabilities for relaxing lanthanide hydrides within the DMFT formalism,
220 built on our recent developments providing DMFT forces for underlying ultra-soft
221 and norm-conserving pseudopotentials, despite the fact that many-body corrections
222 have so far been limited to the electronic contributions to the Eliashberg function. The
223 latter gives structural insights, and we find that many-body effects on the lattice have
224 negligible impacts at high pressures, since DFT structures and pressures are similar to
225 their DMFT counterparts. Although a comprehensive treatment of phonons at the DMFT
226 level is out of reach for such complicated materials, the latter shows that many-body
227 adjustments to the electronic component are responsible for the strong corrections of
228 T_c . We investigated the aliovalent effect and discovered that compared to iso-structural
229 La hydride and Ce hydride, an increase in f character at the Fermi level leads to an
230 increase in superconducting temperature, which is a compelling observation for future
231 explorations of f systems as high T_c superconductors. Our method is general and
232 provides a modular framework for interoperating common first-principles software,
233 such as the freely accessible CASTEP+DMFT and Quantum Espresso codes, with a tiny
234 numerical footprint and ease of implementation.

235 **Author Contributions:** Y.W., F.M., Z.Z., T.T. and E.P. carried out the calculations. All authors
236 wrote the paper. CW designed the research.

237 **Funding:** YW are supported from the China Scholarship Council, CW, NB and EP are supported
238 by the grant [EP/R02992X/1] from the UK Engineering and Physical Sciences Research Council
239 (EPSRC).

240 **Data Availability Statement:** The codes are available at url dmft.ai under the GPL 3.0 license.

241 **Acknowledgments:** This work was performed using resources provided by the ARCHER UK
242 National Supercomputing Service and the Cambridge Service for Data Driven Discovery (CSD3)
243 operated by the University of Cambridge Research Computing Service (www.csd3.cam.ac.uk),
244 provided by Dell EMC and Intel using Tier-2 funding from the Engineering and Physical Sci-
245 ences Research Council (capital grant EP/P020259/1), and DiRAC funding from the Science and
246 Technology Facilities Council (www.dirac.ac.uk).

247 **Conflicts of Interest:** The authors declare no conflict of interest.

References

1. McMillan, P.F. Condensed matter chemistry under 'extreme' high pressure–high temperature conditions. *High Pressure Research* **2004**, *24*, 67–86.
2. Miao, M.; Sun, Y.; Zurek, E.; Lin, H. Chemistry under high pressure. *Nature Reviews Chemistry* **2020**, *4*, 508–527.
3. Wang, H.; Li, X.; Gao, G.; Li, Y.; Ma, Y. Hydrogen-rich superconductors at high pressures. *Wiley Interdisciplinary Reviews: Computational Molecular Science* **2018**, *8*, e1330.
4. Ashcroft, N. Hydrogen dominant metallic alloys: high temperature superconductors? *Physical Review Letters* **2004**, *92*, 187002.
5. Ashcroft, N.W. Metallic hydrogen: A high-temperature superconductor? *Physical Review Letters* **1968**, *21*, 1748.
6. Nakao, H.; Einaga, M.; Sakata, M.; Kitagaki, M.; Shimizu, K.; Kawaguchi, S.; Hirao, N.; Ohishi, Y. Superconductivity of pure H3S synthesized from elemental sulfur and hydrogen. *Journal of the Physical Society of Japan* **2019**, *88*, 123701.
7. Harshman, D.R.; Fiory, A.T. Compressed H3S: inter-sublattice Coulomb coupling in a high- T_c superconductor. *Journal of Physics: Condensed Matter* **2017**, *29*, 445702.
8. Sun, D.; Minkov, V.S.; Mozaffari, S.; Sun, Y.; Ma, Y.; Chariton, S.; Prakapenka, V.B.; Eremets, M.I.; Balicas, L.; Balakirev, F.F. High-temperature superconductivity on the verge of a structural instability in lanthanum superhydride. *Nature Communications* **2021**, *12*, 1–7.
9. Kostrzewa, M.; Szczyński, K.; Durajski, A.; Szczyński, R. From lah 10 to room-temperature superconductors. *Scientific reports* **2020**, *10*, 1–8.
10. Yi, S.; Wang, C.; Jeon, H.; Cho, J.H. Stability and bonding nature of clathrate H cages in a near-room-temperature superconductor LaH 10. *Physical Review Materials* **2021**, *5*, 024801.
11. Li, Y.; Hao, J.; Liu, H.; Li, Y.; Ma, Y. The metallization and superconductivity of dense hydrogen sulfide. *The Journal of chemical physics* **2014**, *140*, 174712.

12. Drozdov, A.; Eremets, M.; Troyan, I.; Ksenofontov, V.; Shylin, S.I. Conventional superconductivity at 203 kelvin at high pressures in the sulfur hydride system. *Nature* **2015**, *525*, 73–76.
13. Drozdov, A.; Kong, P.; Minkov, V.; Besedin, S.; Kuzovnikov, M.; Mozaffari, S.; Balicas, L.; Balakirev, F.; Graf, D.; Prakapenka, V.; others. Superconductivity at 250 K in lanthanum hydride under high pressures. *Nature* **2019**, *569*, 528–531.
14. Kong, P.; Minkov, V.S.; Kuzovnikov, M.A.; Drozdov, A.P.; Besedin, S.P.; Mozaffari, S.; Balicas, L.; Balakirev, F.F.; Prakapenka, V.B.; Chariton, S.; others. Superconductivity up to 243 K in the yttrium-hydrogen system under high pressure. *Nature communications* **2021**, *12*, 1–9.
15. Sun, W.; Kuang, X.; Keen, H.D.; Lu, C.; Hermann, A. Second group of high-pressure high-temperature lanthanide polyhydride superconductors. *Physical Review B* **2020**, *102*, 144524.
16. Liu, L.; Wang, C.; Yi, S.; Kim, K.W.; Kim, J.; Cho, J.H. Microscopic mechanism of room-temperature superconductivity in compressed LaH₁₀. *Physical Review B* **2019**, *99*, 140501.
17. Heil, C.; Di Cataldo, S.; Bachelet, G.B.; Boeri, L. Superconductivity in sodalite-like yttrium hydride clathrates. *Physical Review B* **2019**, *99*, 220502.
18. Song, H.; Zhang, Z.; Cui, T.; Pickard, C.J.; Kresin, V.Z.; Duan, D. High T_c Superconductivity in Heavy Rare Earth Hydrides. *Chinese Physics Letters* **2021**, *38*, 107401.
19. Sarma, S.D.; Li, Q. Many-body effects and possible superconductivity in the two-dimensional metallic surface states of three-dimensional topological insulators. *Physical Review B* **2013**, *88*, 081404.
20. Olalde-Velasco, P.; Jiménez-Mier, J.; Denlinger, J.; Hussain, Z.; Yang, W. Direct probe of Mott-Hubbard to charge-transfer insulator transition and electronic structure evolution in transition-metal systems. *Physical Review B* **2011**, *83*, 241102.
21. Plekhanov, E.; Zhao, Z.; Macheda, F.; Wei, Y.; Bonini, N.; Weber, C. Computational Materials Discovery for Lanthanide Hydrides at high pressure: predicting High Temperature superconductivity. *arXiv preprint arXiv:2107.12316* **2021**.
22. Plekhanov, E.; Bonini, N.; Weber, C. Calculating DMFT forces in ab-initio ultrasoft pseudopotential formalism. *arXiv preprint arXiv:2102.04756* **2021**.
23. Wang, Y.; Lv, J.; Zhu, L.; Ma, Y. CALYPSO: A method for crystal structure prediction. *Computer Physics Communications* **2012**, *183*, 2063–2070.
24. Giannozzi, P.; Baroni, S.; Bonini, N.; Calandra, M.; Car, R.; Cavazzoni, C.; Ceresoli, D.; Chiarotti, G.L.; Cococcioni, M.; Dabo, I.; others. QUANTUM ESPRESSO: a modular and open-source software project for quantum simulations of materials. *Journal of physics: Condensed matter* **2009**, *21*, 395502.
25. Clark, S.J.; Segall, M.D.; Pickard, C.J.; Hasnip, P.J.; Probert, M.I.; Refson, K.; Payne, M.C. First principles methods using CASTEP. *Zeitschrift für Kristallographie-Crystalline Materials* **2005**, *220*, 567–570.
26. Plekhanov, E.; Hasnip, P.; Sacksteder, V.; Probert, M.; Clark, S.J.; Refson, K.; Weber, C. Many-body renormalization of forces in f-electron materials. *Physical Review B* **2018**, *98*, 075129.
27. Lee, H.; Plekhanov, E.; Blackburn, D.; Acharya, S.; Weber, C. The Mott to Kondo transition in diluted Kondo superlattices. *Communications Physics* **2019**, *2*, 1–8.
28. Perdew, J.P.; Burke, K.; Wang, Y. Generalized gradient approximation for the exchange-correlation hole of a many-electron system. *Physical review B* **1996**, *54*, 16533.
29. Perdew, J.P.; Chevary, J.A.; Vosko, S.H.; Jackson, K.A.; Pederson, M.R.; Singh, D.J.; Fiolhais, C. Atoms, molecules, solids, and surfaces: Applications of the generalized gradient approximation for exchange and correlation. *Physical review B* **1992**, *46*, 6671.
30. Rappe, A.M.; Rabe, K.M.; Kaxiras, E.; Joannopoulos, J. Erratum: Optimized pseudopotentials [phys. rev. b 41, 1227 (1990)]. *Physical Review B* **1991**, *44*, 13175.
31. Baroni, S.; De Gironcoli, S.; Dal Corso, A.; Giannozzi, P. Phonons and related crystal properties from density-functional perturbation theory. *Reviews of modern Physics* **2001**, *73*, 515.
32. Dynes, R. McMillan's equation and the T_c of superconductors. *Solid State Communications* **1972**, *10*, 615–618.
33. Allen, P.B.; Dynes, R. Transition temperature of strong-coupled superconductors reanalyzed. *Physical Review B* **1975**, *12*, 905.
34. Weber, C. Unifying guiding principles for designing optimized superconductors. *Proceedings of the National Academy of Sciences* **2021**, *118*.
35. Parcollet, O.; Ferrero, M.; Ayrál, T.; Hafermann, H.; Krivenko, I.; Messio, L.; Seth, P. TRIQS: A toolbox for research on interacting quantum systems. *Computer Physics Communications* **2015**, *196*, 398–415.
36. Aichhorn, M.; Pourovskii, L.; Seth, P.; Vildosola, V.; Zingl, M.; Peil, O.E.; Deng, X.; Mravlje, J.; Kraberger, G.J.; Martins, C.; Ferrero, M.; Parcollet, O. TRIQS/DFTTools: A TRIQS application for ab initio calculations of correlated materials. *Computer Physics Communications* **2016**, *204*, 200–208.

Appendix

Calculated structural parameters of La-H and Ce-H compounds

	Space group	Lattice parameters(Å)	Atoms	Atomic coordinates (fractional)		
				x	y	z
LaH16 (250Gpa)	P6/mmm	a=b=3.52147	H(4h)	0.3333	0.6667	0.1811
		c=3.55630	H(6i)	0.5000	0.0000	0.2522
		$\alpha=\beta=90^\circ$	H(6k)	0.7086	0.0000	0.5000
		$\gamma=120^\circ$	La(1a)	0.0000	0.0000	0.0000

	Space group	Lattice parameters(Å)	Atoms	Atomic coordinates (fractional)		
				x	y	z
CeH16 (250Gpa)	P6/mmm	a=b=3.47980	H(4h)	0.3333	0.6667	0.1754
		c=3.43362	H(6i)	0.5000	0.0000	0.2511
		$\alpha=\beta=90^\circ$	H(6k)	0.2890	0.0000	0.5000
		$\gamma=120^\circ$	La(1a)	0.0000	0.0000	0.0000